

## High Flux and Rejection with Chiral Chitosan Composite Nanofiltration Membranes: Preparation and Characterization

Tao Mu, Yuehua Cong, Baoyan Zhang

Centre for Molecular Science and Engineering, Northeastern University, Shen-Yang 110819, People's Republic of China

Correspondence to: B. Zhang (E-mail: hizklmn1234@163.com) or (E-mail: byzhang2005@126.com)

**ABSTRACT:** Two series of novel composite nanofiltration (NF) membranes were prepared by the overcoating of polysulfone ultrafiltration membranes with a mixture of chitosan and chitosan derivatives modified with two different chiral compounds. The two chiral compounds and their chitosan derivatives were characterized by IR spectroscopy, differential scanning calorimetry, and polarimetry. The structure of the membrane was characterized by scanning electron microscopy (SEM). The rejection and flux of the composite NF membranes were strictly related to the chiral compound grafted to chitosan and its composition in the mixture. An extremely high rejection, 98.23%, was observed with P<sub>2-3</sub> of the polymer (P<sub>2</sub>) composite NF membrane, and the flux remained as high as 351 L m<sup>-2</sup> h<sup>-1</sup> at 0.4 MPa with 1000 mg/L NaCl. These results, together with SEM and IR images of the composite NF membrane, indicated that the chiral compound structure was crucial for the structure and function of the composite membrane. © 2013 Wiley Periodicals, Inc. *J. Appl. Polym. Sci.* 129: 3582–3590, 2013

**KEYWORDS:** crosslinking; grafting; membranes

Received 12 July 2012; accepted 15 October 2012; published online 1 March 2013

DOI: 10.1002/app.38734

### INTRODUCTION

Nanofiltration (NF), a type of separation membrane technology between reverse osmosis and ultrafiltration (UF) with high efficiency and low energy expenditure, has been actively studied over the years. NF membranes have been applied in many fields, including the water-softening treatment of wastewater, food processing, medicine, and the oil industry.<sup>1–3</sup> However, the conventional NF membrane restricts itself in that it cannot maintain a high electrolyte rejection with a high flux. A severe decline in the flux over an extended period of operation is often observed.<sup>4,5</sup> To solve this major issue, many approaches have been reported; these approaches can be classified into two classes: altering the membrane structures or improving membrane preparation process. The first approach was exploited in this study. The membrane properties were altered by the adjustment of the membrane composition with chitosan and its derivatives. Chitosan, a cationic polysaccharide obtained by the alkaline *N*-deacetylation of chitin, has been routinely used in membrane preparation because of its abundance, hydrophilicity, and environmental benignancy.<sup>4,6</sup> By hydroxylation, amination reactions in chitosan can be modified.<sup>7–12</sup> With the use of chitosan and its modified derivatives, various NF membranes have been reported and prepared by different preparation methods, such as surface crosslinking, blending, and ultraviolet irradiation.<sup>9–13</sup>

Composite NF membrane based on composite structures were designed in this study, with a polysulfone UF membrane as the base to provide mechanical strength and a modified chitosan/chitosan mixture as the top layer to provide the filtration function; our aim was to achieve a high rejection and maintain a high flux. As helical structures exist in chiral compounds,<sup>14–18</sup> two chiral compounds with such structures were grafted onto chitosan through hydroxylation in this study to change the structure and, hence, the performance of the NF membrane. Two series of NF membranes were prepared with the mixture of chitosan and the chitosan modified with the two chiral compounds. The structures of the chiral compounds had a big impact on the NF composite membrane properties. As a result, the rejection of one composite NF membrane for NaCl was improved, and the flux was about three times higher than that reported previously.<sup>12,19–21</sup>

### EXPERIMENTAL

#### Materials and Methods

A self-made testing instrument was adopted for the membrane performance test, as shown in Figure 1. A DDS-307 conductivity meter (Shanghai China Leici Instrument Factory) was used to evaluate the conductivity of solution. A Spectrum One IR spectrometer (PerkinElmer) was used to test the chemical compositions of the monomers and polymers. A differential

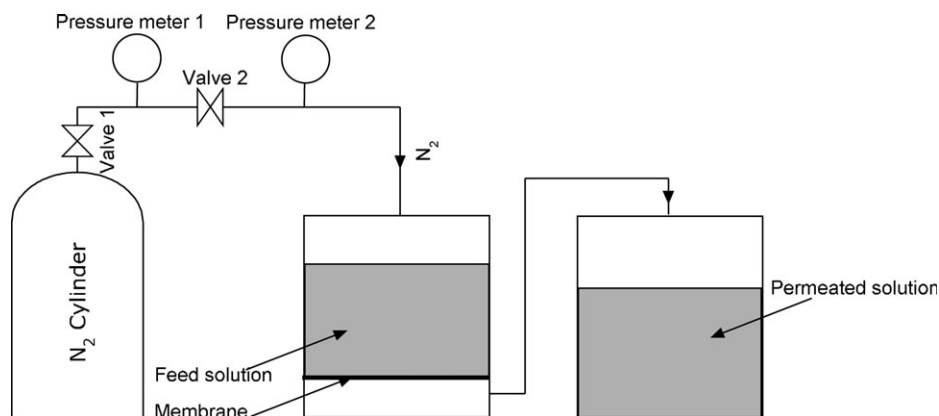


Figure 1. Diagram of the experimental apparatus for testing of the rejection and flux.

scanning calorimetry (DSC) analytical meter (Netzsch DSC-204) was used to measure the thermal transition properties of the monomers. A PerkinElmer 341 polarimeter was used to performed the optical rotation of the monomers. An SSX-550 type scanning electron microscope (Shimadzu) was used to observe the morphology of the NF membrane, and a Spotlight 300 IR imaging system (PerkinElmer) was used to measure the distribution of the functional layers on the surface of the substrate layer.

Chitosan (weight-average molecular weight  $\geq 20,000$  Da, degree of deacetylation  $\geq 90\%$ ), succinic anhydride, 4-dimethylaminopyridine, menthol, and *N*-methyl pyrrolidone were all analytical grade and were purchased from Shanghai China Sinopharm Chemical Reagent Co., Ltd. Hexanedioic acid, glutaraldehyde, poly(vinyl alcohol), acetone, and  $\text{SOCl}_2$  were purchased from Shenyang China Xinxin Reagent Factory. Acetic acid was purchased from Shantou China Xilong Chemical Co., Ltd. Cholesterol was purchased from Henan China Xiayi Bell Biological Products Co., Ltd., and polysulfone was purchased from Shanghai China Shuguang Chemical Plastics Industrial Corp.

### Preparation of the Modified Chitosan

**Structure of the Two Chiral Compounds.** The chiral compounds  $M_1$  and  $M_2$  were prepared according to a procedure of the literature,<sup>22,23</sup> and their structures are shown in Figures 2 and 3.

**Polymerization Schemes.** Chitosan was grafted with two monomers with different molar ratios, and the polymerization schemes are shown in Figures 4 and 5.

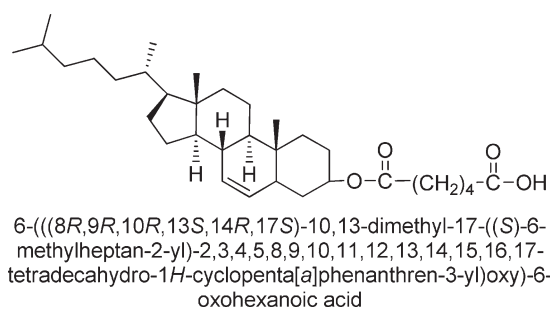


Figure 2. Structure of monomer  $M_1$ .

**General Procedure for the Preparation of the Chiral-Compound-Modified Chitosan.** The acid chloride derivatives of  $M_1$  and  $M_2$  were prepared by the reaction of  $M_1$  and  $M_2$  with  $\text{SOCl}_2$  at  $50^\circ\text{C}$  for 6 h. The products were purified by distillation.

The acyl chlorides obtained from the last step were dissolved in chloroform and added to the chitosan methane sulfonic acid solution dropwise. Once the addition was completed, the mixture was allowed to react for 3.5 h. The ratios between chitosan and  $M_1$  or  $M_2$  acyl chloride are listed in Tables I and II. Once the reaction was over, the reaction mixture was cooled down to  $4^\circ\text{C}$  for 10 h before precipitation treatment with acetone. The products were then filtered twice and allowed to dry *in vacuo*.

### Preparation of the UF Membranes

The polysulfone UF membrane was prepared by the phase-inversion method. The procedure was as follows:<sup>24–27</sup> 4.2 g of polysulfone was dissolved in 25.7 g of *N*-methylpyrrolidone. To this solution was added 0.12 g of acetone and 0.075 g of polyvinylpyrrolidone (PVP) to form the casting solution, which was filtered through a G2 sand filter to remove the undissolved impurities. The solution was then allowed to deaerate by standing still for 10 h.

The casting solution was coated on a piece of gauze (80 hole) tiled on the glass ( $10 \times 10 \text{ cm}^2$ ) with a glass rod. The solvent in the membrane was first partially evaporated at ambient temperature for a minute, and then, the membrane was transferred to a water bath to set.

### Preparation of the Composite NF Membranes

Chitosan modified with chiral compound  $M_1$  or  $M_2$  (0.03 g) and chitosan (0.06 g) were dissolved in 2.5 mL of a 4% acetic acid solution with 0.04% poly(vinyl alcohol) (porogen). The

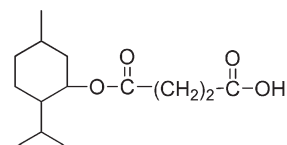


Figure 3. Structure of monomer  $M_2$ .

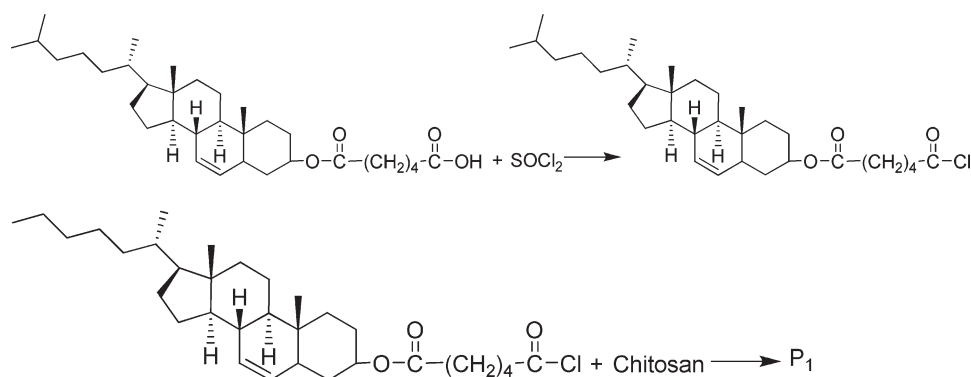


Figure 4. Scheme of polymer P<sub>1</sub> synthesis.

chitosan casting solution was obtained by deaeration with the previous solution.

The polysulfone UF membrane was first fixed on the glass (10 × 10 cm<sup>2</sup>). The chitosan casting solution was then spread onto the UF membrane. The newly formed membrane was vaporized for 1 min at room temperature and then crosslinked by the application of 1% glutaraldehyde onto it. The composite membrane was ready after 16 h at ambient temperature.

To investigate the effect of the membrane preparation conditions on the performance, a series of NF membranes were prepared under different conditions.

#### Permeation Experiment

The tests of the composite NF membrane were conducted with the self-made test equipment shown in Figure 1 at a prepressure of 0.4 MPa for 0.5 h.

Flux and rejection were calculated with eqs. (1) and (2), respectively:<sup>19,21,28</sup>

$$F = V/At \quad (1)$$

where  $F$  is the flux,  $V$  is the volume of the permeating fluid passing through the membrane,  $A$  is the effective area of membrane (0.93 cm<sup>2</sup>), and  $t$  is the time for permeation.

$$R = (1 - C_p/C_0) \times 100\% \quad (2)$$

where  $R$  is the rejection and  $C_p$  and  $C_0$  are the concentrations of the permeate fluid and the feed, respectively.

The concentration was replaced by the conductivity of salt solutions because the 1000 mg/L of inorganic salt solution could be deemed

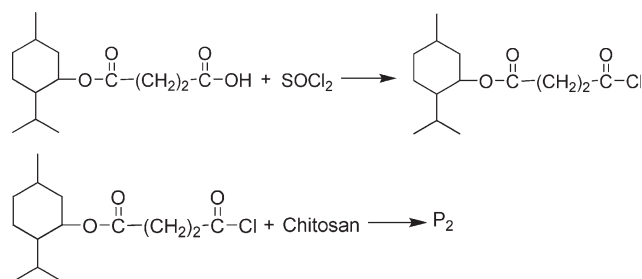


Figure 5. Scheme of polymer P<sub>2</sub> synthesis.

an extremely dilute solution for this study. The DDS-307 conductivity meter was used to evaluate the conductivity of solution.

## RESULTS AND DISCUSSION

### Characterization of the Chiral Compounds and the Chitosan Derivatives

The Spectrum One IR spectrometer was used to test the chemical compositions of the chiral compounds and the chitosan derivatives.

The IR spectrum of M<sub>1</sub> is shown in Figure 6. The absorption band at 3433 cm<sup>-1</sup> was associated with the stretching vibration of the hydroxyl of carboxylic acid; the absorption bands at 2943 and 2867 cm<sup>-1</sup> were associated with the stretching vibrations of methyl and methylene, and the absorption bands at 1722 and 1694 cm<sup>-1</sup> were associated with the stretching vibrations of carbonyl.

The IR spectrum of M<sub>2</sub> is shown in Figure 7. The absorption band at 3500 cm<sup>-1</sup> was associated with the stretching vibrations of hydroxyl of carboxylic acid. The absorption band at 3079–2854 cm<sup>-1</sup> was associated with the stretching vibrations of carboxylic acid and hydroxyl. The absorption band at 2959–2874 cm<sup>-1</sup> was associated with the stretching vibrations of saturated hydrocarbon. The absorption band at 2642–2530 cm<sup>-1</sup> was associated with the stretching vibrations of carboxyl, and the absorption band at 1708 cm<sup>-1</sup> was associated with the stretching vibrations of carboxylic acid carbonyl.

Table I. Polymer (P<sub>1</sub>) Grafting Reaction Feeding

Polymer (P <sub>1</sub> )	$m_{cts}$ (g)	$m_{M1}$ (g)	$B$
P <sub>1-0</sub>	1.09	0	0
P <sub>1-1</sub>	1.09	0.026	0.01
P <sub>1-2</sub>	1.09	0.051	0.02
P <sub>1-3</sub>	1.09	0.129	0.05
P <sub>1-4</sub>	1.09	0.257	0.1
P <sub>1-5</sub>	1.09	0.514	0.2
P <sub>1-6</sub>	1.09	1.258	0.5
P <sub>1-7</sub>	1.09	2.056	0.8
P <sub>1-8</sub>	1.09	2.57	1.0

$m_{cts}$ , Mass of Chitosan;  $m_{M1}$ , Mass of M<sub>1</sub>;  $B$ , molar ratio of the primary hydroxyl and monomer M<sub>1</sub>.

**Table II.** Polymer (P<sub>2</sub>) Grafting Reaction Feeding

Polymer (P <sub>2</sub> )	m <sub>cts</sub> (g)	m <sub>M2</sub> (g)	B
P <sub>2-0</sub>	1.09	0	0
P <sub>2-1</sub>	1.09	0.011	0.01
P <sub>2-2</sub>	1.09	0.023	0.02
P <sub>2-3</sub>	1.09	0.057	0.05
P <sub>2-4</sub>	1.09	0.114	0.1
P <sub>2-5</sub>	1.09	0.228	0.2
P <sub>2-6</sub>	1.09	0.570	0.5
P <sub>2-7</sub>	1.09	0.912	0.8
P <sub>2-8</sub>	1.09	1.140	1.0

m<sub>cts</sub>, Mass of Chitosan; m<sub>M2</sub>, Mass of M2; B, molar ratio of the primary hydroxyl and monomer M<sub>2</sub>.

As shown in Figures 8 and 9, compared to those of the raw chitosan (the bottom), the ester carbonyl absorption peak appeared at 1730 cm<sup>-1</sup>, and the absorption peak of ester carbonyl increased with increasing ratio of monomer and the primary hydroxyl of chitosan from bottom to top. M<sub>1</sub> and M<sub>2</sub> were grafted onto chitosan successfully.

**Thermal Analysis.** The phase transitions and corresponding enthalpy changes of the chiral compounds were characterized by DSC.

The DSC curve of monomer M<sub>1</sub> is shown in Figure 10. The heating curve had two endothermic peaks, which corresponded to the melting temperature ( $T_m = 137^\circ\text{C}$ ) and the clear point ( $T_i = 147^\circ\text{C}$ ), respectively, and the endothermic enthalpies of which were  $\Delta H_m = 72.37 \text{ J/g}$  and  $\Delta H_i = 1.15 \text{ J/g}$ .

The DSC curve of monomer M<sub>2</sub> is shown in Figure 11. The heating curve had single endothermic peaks:  $T_m$  ( $T_m = 67^\circ\text{C}$ ) and endothermic enthalpy ( $\Delta H_m = 85.49 \text{ J/g}$ ).

**Optical Rotation.** The optical rotation of the monomers was performed by the PerkinElmer 341 polarimeter. M<sub>1</sub> and M<sub>2</sub>

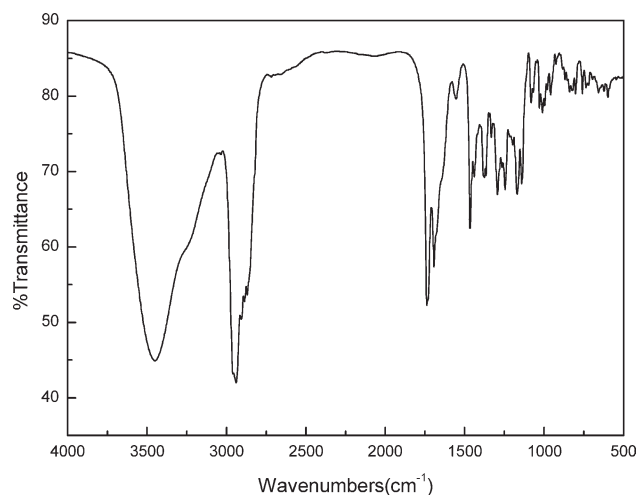


**Figure 6.** IR spectrum of M<sub>1</sub>.

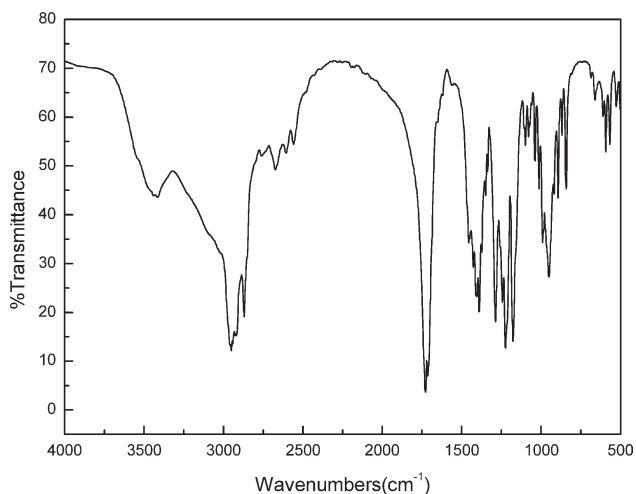


**Figure 7.** IR spectrum of M<sub>2</sub>.

were optically active in the light of a Na lamp at  $\lambda = 589 \text{ nm}$  at ambient temperature.

At ambient temperature, the optical rotations of the chiral monomers M<sub>1</sub> and M<sub>2</sub> are shown in Table 3. M<sub>1</sub> and M<sub>2</sub> were chiral and had helical structures.

The following conclusion could be drawn from the analysis: M<sub>1</sub> and M<sub>2</sub> were respectively grafted onto chitosan. They were chiral compounds in which helical structures existed.<sup>16–18</sup>

#### Effects of the Degree of Modification of Chitosan by Different Monomers on the Rejection and Flux of the Composite NF Membranes

Tests of the two series of composite NF membranes were conducted after a prepressure at 0.4 MPa for 0.5 h. Each membrane with a different grafting ratio was tested three times, and the flux and rejection values are shown in Figures 12–15. Not much difference in the flux and rejection values with different salts were observed. The order of the flux was as follows: Pure water > NaCl > Na<sub>2</sub>SO<sub>4</sub> ≈ CaCl<sub>2</sub>. The reason for this may have been

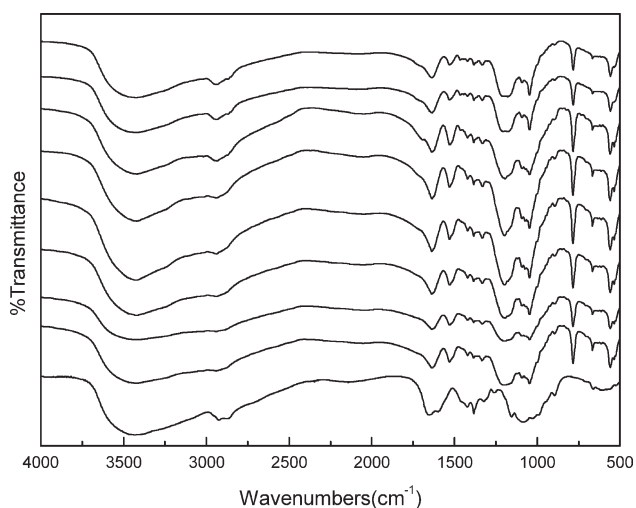


**Figure 8.** IR spectrum of polymer P<sub>1</sub>.

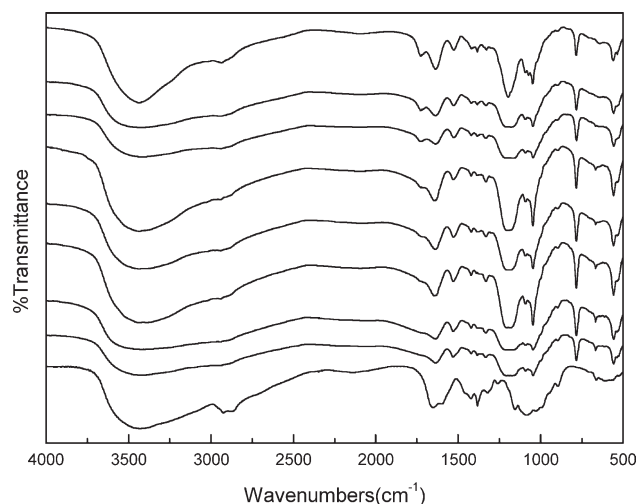


Figure 9. IR spectrum of polymer P<sub>2</sub>.

the effect of the membrane's rejection to the salt. The order of rejection was as follows: Na<sub>2</sub>SO<sub>4</sub> ≈ CaCl<sub>2</sub> > NaCl. This was due to the sizes of the particles. The rejection and flux values of the NF membrane with chiral compound M<sub>1</sub> both increased up to 5% in the P<sub>1-3</sub> composite membrane. The maximum rejection values [64.4% (NaCl), 65.8% (Na<sub>2</sub>SO<sub>4</sub>), and 65.6% (CaCl<sub>2</sub>)] were observed with P<sub>1-4</sub> when the grafting degree of M<sub>1</sub> to chitosan was 10% and the corresponding flux was about 2104–2856 L m<sup>-2</sup> h<sup>-1</sup>. The data indicated that the structure of M<sub>1</sub> and its grafting percentages in the chitosan derivative were crucial for the composite membrane performance. When the grafting degree was higher than 10%, the rejection dropped, and the flux increased; this suggested that the filtration performance was deteriorating. The phenomena might be explained as follows: with the right percentage, the helical structure of M<sub>1</sub> made the tortuosity of the pore increase. The pore became larger when the percentage exceeded 10%, this might have resulted from the volume. The NF membrane with M<sub>2</sub> showed 97.1% (NaCl), 97.8% (Na<sub>2</sub>SO<sub>4</sub>), and 97.7% (CaCl<sub>2</sub>) values of maximum rejection and 349–371 L m<sup>-2</sup> h<sup>-1</sup> corresponding flux values when the grafting degree was 5% (P<sub>2-3</sub>). The M<sub>1</sub> and M<sub>2</sub>

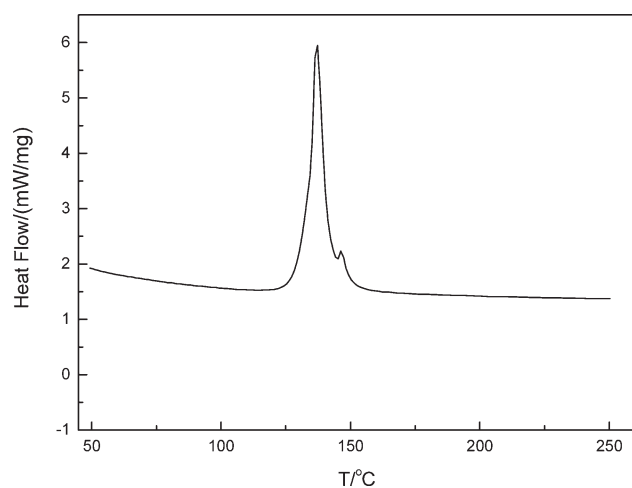


Figure 10. Heating DSC curve of M<sub>1</sub> (T = temperature).

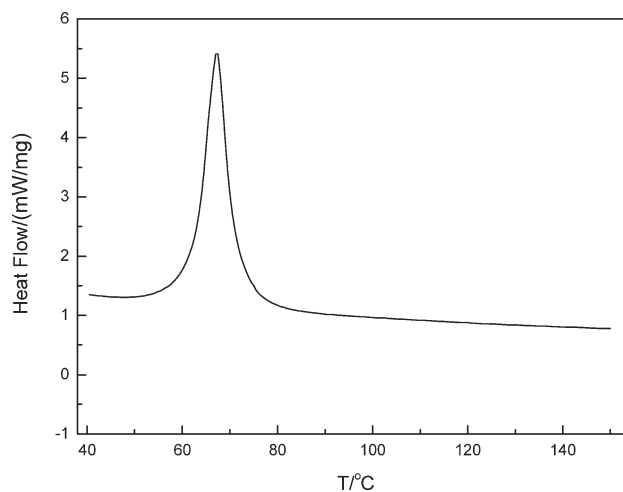


Figure 11. Heating DSC curve of M<sub>2</sub> (T = temperature).

had chiral carbon atoms, which resulted in the formation of the helical structures of M<sub>1</sub> and M<sub>2</sub>. The M<sub>1</sub> molecular weight (514) was much larger than that of M<sub>2</sub> (256), and the volume of M<sub>1</sub> was also larger than that of M<sub>2</sub>. Although it shared a similar structure with M<sub>1</sub>, M<sub>2</sub> was smaller in size, and a more tortuous path in the membrane with M<sub>2</sub> was required, so the rejection was much higher. P<sub>2-3</sub> was selected as the casting material. The latter test of the rejection and flux was performed with an NaCl solution because the differences were very small between solutions of different salts.

#### Effect of the Membrane Preparation Conditions on the Performance of the NF Membranes

**Effect of the Glutaraldehyde Concentration on the Rejection and Flux of the Composite NF Membranes.** The NF membranes were prepared with different concentrations of glutaraldehyde solution (0.1, 0.2, 0.5, 0.75, 1, 1.25, 1.5, 1.75, and 2%) as a crosslinking agent. The effect of the glutaraldehyde concentration on the performance of the composite membranes is shown in Figure 16. The increase in the rejection with decreasing flux was observed as the concentration of glutaraldehyde was increased from 0 to 1.25%. Once the concentration was higher than 1.25%, a sharp drop in the rejection and a substantial increase in the flux resulted. The reason may have been that the crosslinking reaction occurred in the surface at low concentration, which made the surface of the membrane compact. The crosslinking reaction occurred in the whole active layer when the glutaraldehyde concentration increased to 1.25%; this led to the formation of a larger net structure and an increase in the size of the apertures. Thus, the rejection decreased, and the flux increased.<sup>20,29</sup> The maximum rejection was 98.1% with the flux at 351.4 L m<sup>-2</sup> h<sup>-1</sup> at the optimum concentration of the glutaraldehyde of 1.25%.

Table III. Optical Rotation of the Monomers

Monomer	Optical rotation (°)
M <sub>1</sub>	-2.4 ± 0.3
M <sub>2</sub>	+0.005 ± 0.001



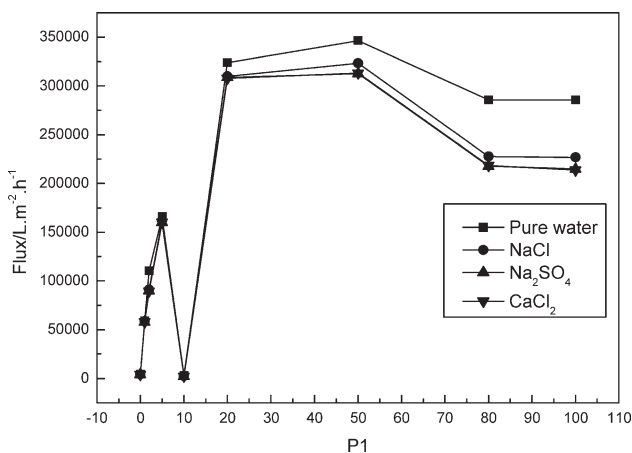


Figure 12. Flux of the P<sub>1</sub> composite membrane.

**Effect of the Poly(vinyl alcohol) Concentration on the Rejection and Flux of the Composite NF Membrane.** The membranes were prepared with different concentrations of poly(vinyl alcohol) solution (0.01, 0.02, 0.04, 0.06, 0.08, 0.1, and 0.12%). The effect of the poly(vinyl alcohol) concentration is shown in Figure 17. The impact of the poly(vinyl alcohol) concentration on the rejection was not very significant. With 0.06% poly(vinyl alcohol), the flux reached as high as 351 L m<sup>-2</sup> h<sup>-1</sup>, while a good rejection of 98.1% was maintained. The pore ratio increased along with the increasing concentration; this resulted in an increased flux with decreased rejection. However, poly(vinyl alcohol) was not dissolved completely when its concentration exceeded 0.06%, and the flux and rejection maintained stable. A poly(vinyl alcohol) concentration of 0.06% was selected.

**Effect of the Acetic Acid Concentration on the Rejection and Flux of the Composite NF Membrane.** The membranes were prepared with the following concentrations of acetic acid: 1, 2, 3, 4, 5, 6, 7, 8, and 9%. The effect of the acetic acid concentration is shown in Figure 18. The rejection increased at first and then decreased, whereas the flux first decreased and then

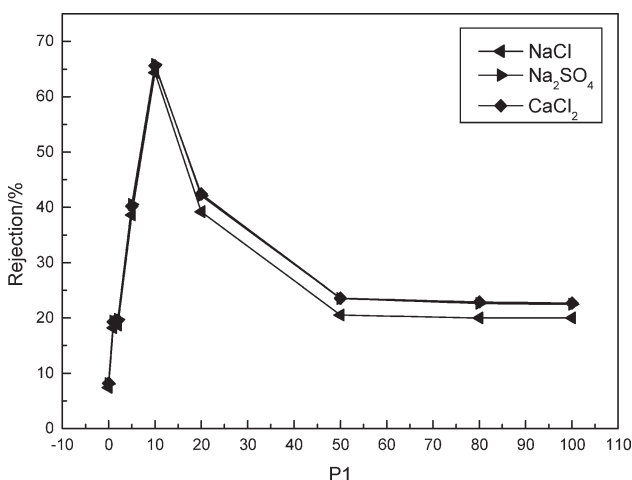


Figure 13. Rejection of the P<sub>1</sub> composite membrane.

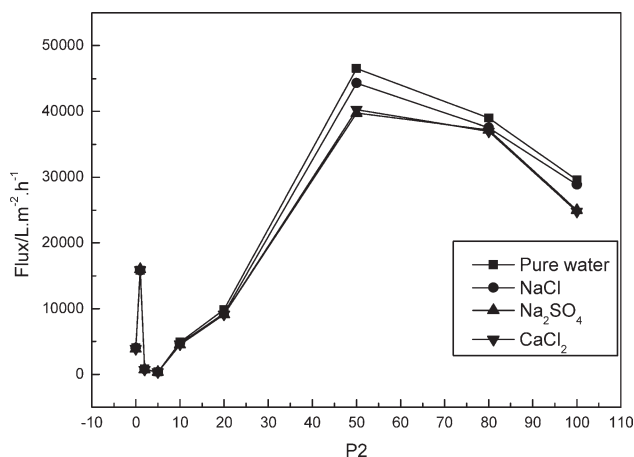


Figure 14. Flux of the P<sub>2</sub> composite membrane.

increased. With 5% acetic acid, the maximum rejection was 98.14%, and the corresponding flux was 351 L m<sup>-2</sup> h<sup>-1</sup>. The reason for this may have been that the chitosan was not dissolved in pure water, whereas in acetic acid, the chitosan dissolved gradually with increasing acetic acid concentration. A more uniform film was formed, so the flux decreased with increasing rejection. Chitosan was dissolved completely when the concentration was 5%. A higher concentration of acid might have led to the decomposition of chitosan and its derivatives; subsequently, the porosity increased, the flux increased, and the rejection decreased. Therefore, 5% was the optimum concentration of acetic acid.

**Effect of the Crosslinking Time on the Rejection and Flux of the Composite NF Membranes.** The effect of different crosslinking times on the performance of the NF composite membranes was also investigated. A series of composite NF membranes were prepared with different linking times of 10, 12, 14, 16, 18, 20, 22, 24, and 26 h. The effect of the crosslinking time is shown in Figure 19. When the crosslinking time was extended from 10 to 18 h, an increase in the rejection with decreasing flux was observed. Once the crosslinking time was

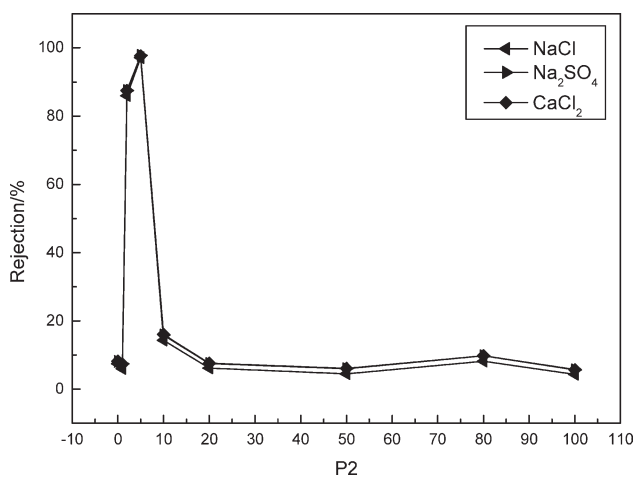
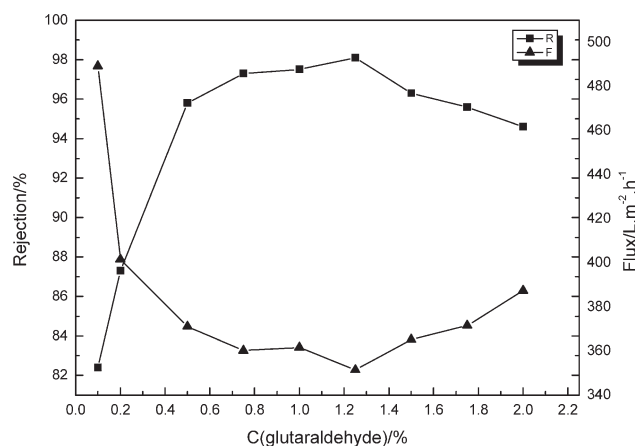


Figure 15. Rejection of the P<sub>2</sub> composite membrane.



**Figure 16.** Effect of the glutaraldehyde concentration ( $C$ ) on the rejection and flux of the composite membranes.

elongated further, the opposite effect was observed. The reason might have been that the pore contraction and tortuosity increased with increasing crosslinking degree when the crosslinking occurred for less than 18 h. When the crosslinking time was prolonged, the Schiff base might have been degenerative because of the breakage of the  $C=N$  bond.<sup>19,30</sup> Therefore, the optimal crosslinking time was 18 h.

**Effect of the Ratio between  $P_{2-3}$  and the Chitosan on the Rejection and Flux of the Composite NF Membranes.** The impact of the ratio between chitosan and its chiral derivative  $P_{2-3}$  was the most significant on the membrane properties. A series of composite NF membranes were prepared and characterized with  $P_{2-3}$ /chitosan ratios of 0 : 9, 1 : 8, 2 : 7, 3 : 6, 4 : 5, 5 : 4, 6 : 3, 7 : 2, and 8 : 1. As shown in Figure 20, the rejection increased first and then decreased; the flux increased slightly after increasing sharply at first. The  $P_{2-3}$  was water soluble and its volume was large; it attached to the wall of pore at the beginning; as a result, the flux declined, and the rejection increased. When the proportion of  $P_{2-3}$  increased to a certain level and the proportion of chitosan was correspondingly

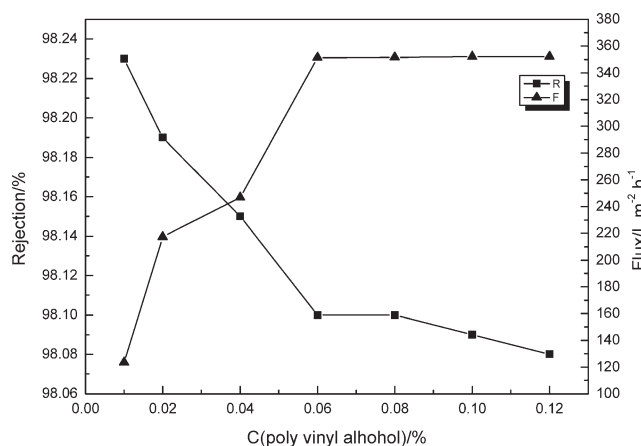


**Figure 17.** Effect of the poly(vinyl alcohol) concentration ( $C$ ) on the rejection and flux of the composite membrane.

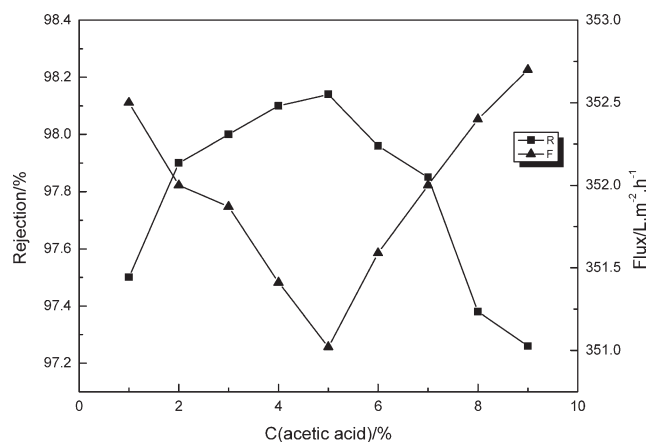


**Figure 18.** Effect of the acetic acid concentration ( $C$ ) on the rejection and flux of the composite membrane.

reduced, it was hard to form a film on the base membrane. The size of the pore was at the level of UF, so the flux increased, and the rejection decreased. When the proportion of  $P_{2-3}$  was increased continuously, it could not form a film on the polysulfone surface. The phenomena of adsorption no longer occurred. As a result, the aperture size did not change. The flux and rejection stabilized at the same time. Therefore, the optimal ratio was 3 : 6.

On the basis of previous results, the best experimental conditions for the composite membrane preparation were derived as follows: the glutaraldehyde concentration was 1.25%, the poly(vinyl alcohol) concentration was 0.06%, the acetic acid concentration was 5%, the crosslinking time was 18 h at room temperature, and the ratio of  $P_{2-3}$  to chitosan was 3 : 6. Under these conditions, the rejection was 98.23%, and the flux was  $351 \text{ L m}^{-2} \text{ h}^{-1}$  with 1000 mg/L NaCl.

#### Characterization of the Composite Membrane Structure

The cross section and surface of this membrane were characterized by an SSX-550 scanning electron microscope, as shown in Figure 21. The composite membrane surface was magnified by

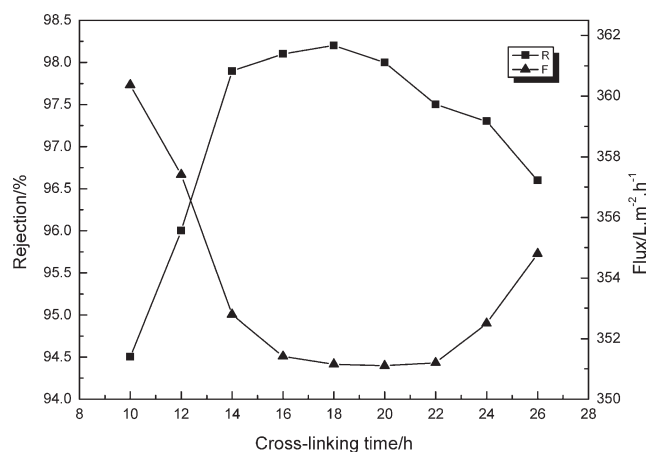


**Figure 19.** Effect of the crosslinking time on the rejection and flux of the composite membrane.

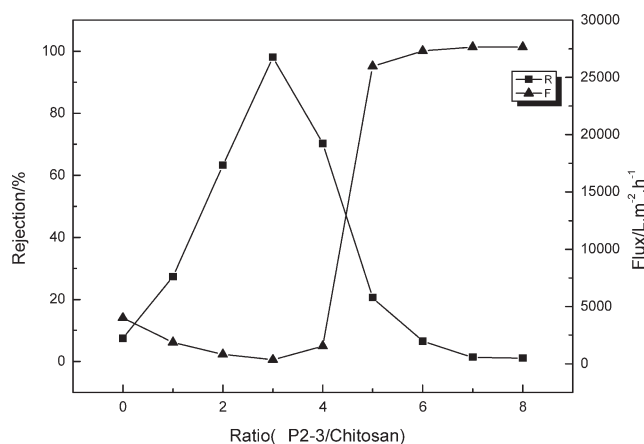


**Figure 20.** Effect of the ratio between P<sub>2-3</sub> and the chitosan on the rejection and flux of the composite membrane.

20,000 and 3000, as shown in Figure 21(a,b). The surface of the composite membrane was compact yet uneven and formed the active layer of the composite membrane. The cross section of the composite membrane had two layers; the upper was a thin and dense crosslinking layer, and the lower was the polysulfone support layer with a fingerlike, pore-rich structure.

#### IR Imaging Analysis of the Composite Membrane Surface

The homogeneity of the prepared NF composite membranes was investigated by IR imaging analysis, as shown in Figure 22. The blue zone (in the online figure) represents the polysulfone membrane layer and corresponds to the characteristic peak at 1252.50 cm<sup>-1</sup>, with the gray representing chitosan and corresponding to the characteristic peak at 1653.88 cm<sup>-1</sup>. The white zone represents the modified chitosan and corresponds to the characteristic peak at 1731.32 cm<sup>-1</sup>. Together, they constituted the functional layer. The modified chitosan and chitosan were distributed evenly on the surface of the polysulfone membrane, as revealed by the homogeneous appearance of the white and gray zones distributed in the blue background.

#### CONCLUSIONS

The composite nanofiltration membranes reported in this article were structured with two layers: the upper one was the

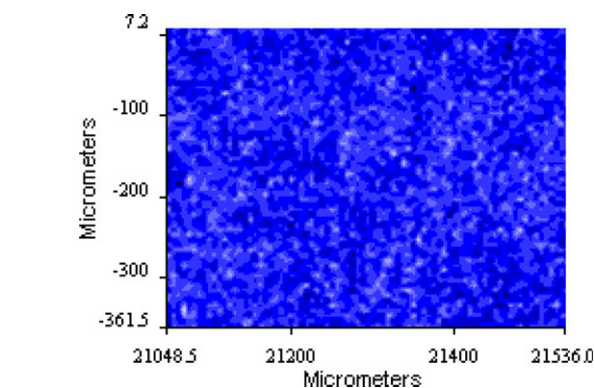


**Figure 22.** IR imaging of the composite membrane surface. [Color figure can be viewed in the online issue, which is available at [wileyonlinelibrary.com](http://wileyonlinelibrary.com).]

thin and dense crosslinked layer, which played a crucial role in separation, and the lower layer was the polysulfone support layer, with a spongelike porous texture. The upper layer was prepared with a homogeneous mixture of chiral-compound-modified chitosan and chitosan, as revealed by the IR image analysis. With the optimal composite membrane preparation conditions [1.25% glutaraldehyde concentration, 0.06% poly (vinyl alcohol) concentration, 5% acetic acid concentration, 18 h crosslinking time at room temperature, and P<sub>2-3</sub>/chitosan ratio of 1 : 2], the rejection of the membrane was 98.23% with a flux as high as 351 L m<sup>-2</sup> h<sup>-1</sup> with 1000 mg/L NaCl. These excellent high flux and rejection values were the result of the membrane structure and function modification through the introduction of the chiral compounds M<sub>1</sub> and M<sub>2</sub>. Both of the compounds had distinct structures. An increasing flux with a relatively high rejection was observed with the M<sub>1</sub>-modified chitosan composite membrane. The best performance was achieved with the composite membrane with P<sub>2-3</sub> with M<sub>2</sub>. The resulting NF composite membrane allowed high flux with very high rejection. Further study of this unique membrane is ongoing. This work might open the possibility of improving NF membrane properties through the introduction of novel compounds.

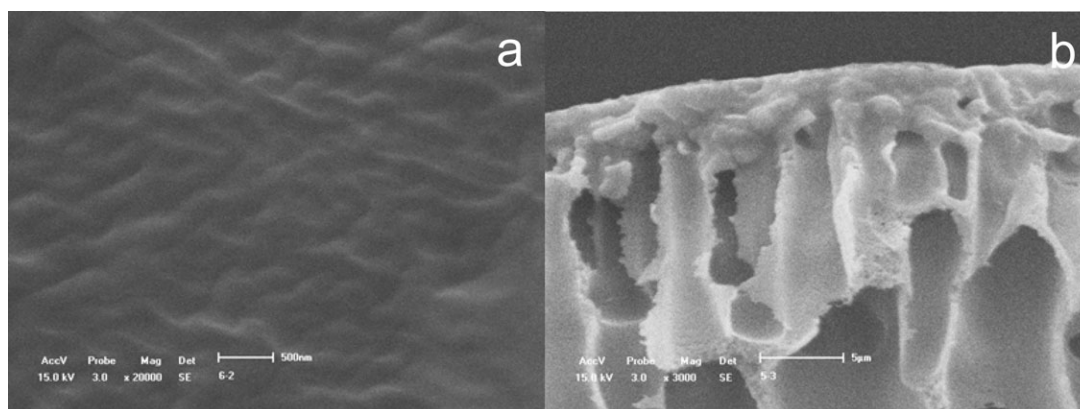


**Figure 21.** (a) Surface and (b) cross section images of the composite membrane.



## ACKNOWLEDGMENTS

The authors acknowledge financial support from the National Key Technology Support Program of China (contract grant number 2008BAL55B03).

## REFERENCES

1. Gao, A. M.S. Thesis, Zhengzhou University, **2002**.
2. Gao, C.; Chen, Y. *TNMSC* **2004**, *14*, 310.
3. Wang, Z. *Fundamentals of Membrane Separation Technique*; Chemical industry press: Beijing China, **2000**; p 1.
4. Yoon, K.; Kim, K.; Wang, X.; Fang, D.; Hsiao, B. S.; Chu, B. *Polymer* **2006**, *47*, 2434.
5. Li, X.-L.; Zhu, L.-P.; Zhu, B.-K.; Xu, Y.-Y. *Sep. Purif. Technol.* **2011**, *83*, 66.
6. Boricha, A. G.; Murthy, Z. V. P. *J. Appl. Polym. Sci.* **2008**, *110*, 3596.
7. Sun, L.; Qi, J.; Ge, H. *Chem. Equip. Technol.* **2004**, *25*, 8.
8. Zhu, Y. M.S. Thesis, Ocean University of China, **2007**.
9. Xu, C.; Lu, C.; Ding M. *J. Funct. Polym.* **1997**, *10*, 51.
10. Huang, R.; Chen, G.; Wang, J. *Mod. Chem. Ind.* **2006**, *26*, 204.
11. Huang, R.-H.; Chen, G.-H.; Sun, M.-K.; Hu, Y.-M.; Gao, C.-J. *Carbohydr. Polym.* **2007**, *70*, 318.
12. Huang, R.; Chen, G.; Sun, M.; Gao, C. *Sep. Purif. Technol.* **2008**, *58*, 393.
13. Marconnet, C.; Houari, A.; Seyer, D.; Djafer, M.; Coriton, G.; Heim, V.; Di Martino P. *Desalination* **2011**, *276*, 75.
14. Zhou, Q.; Wang, X. *Liquid Crystal Polymer*; Science Press: Beijing, **1994**; p 1.
15. He, T.; Hu, H. *Functional Polymer and New Technology*; Chemical Industry Press: Beijing, **2001**; p 241.
16. Wu, D.; Xie, X.; Xu, J. *Polymer Liquid Crystals*; Sichuan Education: Chengdu, **1988**; p 10.
17. Lin, J. *Fundamentals of Steroid Chemistry*; Chemical Industry Press: Beijing, **1989**; p 22.
18. Ye, X. *Stereochemistry*; Peking University Press: Beijing, **1999**; p 270.
19. Huang, R.; Chen, G.; Sun, M.; Gao, C. *Carbohydr. Res.* **2006**, *341*, 2777.
20. Miao, J.; Chen, G. H.; Gao, C. *J. Desalination* **2005**, *181*, 173.
21. Li, L. C.; Wang, B. G.; Tan, H. M.; Chen, T. L.; Xu, J. P. *J. Membr. Sci.* **2006**, *269*, 84.
22. Cong, Y.-H.; Wang, W.; Tian, M.; Meng, F.-B.; Zhang, B.-Y. *Liq. Cryst.* **2009**, *36*, 455.
23. Yan, R.; Chen, L.; Huang, X.; Zhang, G.; Huang C. *Food Ferment. Ind.* **2008**, *34*, 89.
24. Marcel, M. *Basic Principles of Membrane Technology*; Tsinghua University Press: Beijing, **1999**; p 191.
25. Mosqueda-Jimenez, D. B.; Narbaitz, R. M.; Matsuura, T. *Sep. Purif. Technol.* **2004**, *37*, 51.
26. Mosqueda-Jimenez, D. B.; Narbaitz, R. M.; Matsuura, T.; Chowdhury, G.; Pleizier, G.; Santerre, J. P. *J. Membr. Sci.* **2004**, *231*, 209.
27. Ma, Y.; Shi, F.; Ma, J.; Wu, M.; Zhang, J.; Gao, C. *Desalination* **2011**, *272*, 51.
28. Song, Y. J.; Liu, F.; Sun, B. H. *J. Appl. Polym. Sci.* **2005**, *95*, 1251.
29. Musale, D. A.; Kumar, A. *Sep. Purif. Technol.* **2000**, *21*, 27.
30. Huang, R.; Chen, G.; Yang, B.; Gao, C. *Sep. Purif. Technol.* **2008**, *61*, 424.